



# Multipurpose fluorescent carbon dots from papaya seed waste as sensing materials for Cu<sup>2+</sup> detection and diethyl ether vapor sensor via electronic nose system

Nichaphat THONGSAI<sup>1</sup>, Aphinya CHUIDUANG<sup>2</sup>, Sumana KLADSOMBOON<sup>3</sup>, Insik IN<sup>4,5</sup>, and Peerasak PAOPRASERT<sup>2,\*</sup>

<sup>1</sup> Department of Chemistry, Faculty of Science, Ramkhamhaeng University, Ramkhamhaeng Road, Bang Kapi, Bangkok, 10240, Thailand

<sup>2</sup> Department of Chemistry, Faculty of Science and Technology, Thammasat University, Phaholyothin Road, Klong Luang, Pathumthani, 12120, Thailand

<sup>3</sup> Department of Radiological Technology, Faculty of Medical Technology, Mahidol University, Nakhon Pathom, 73170, Thailand

<sup>4</sup> Department of IT Convergence (Brain Korea PLUS 21), Korea National University of Transportation, Chungju 380-702, South Korea

<sup>5</sup> Department of Polymer Science and Engineering, Korea National University of Transportation, Chungju 380-702, South Korea

\*Corresponding author e-mail: peerasak@tu.ac.th

## Received date:

21 March 2023

## Revised date:

14 June 2023

## Accepted date:

21 June 2023

## Keywords:

Carbon dots;

Papaya seed;

Cu<sup>2+</sup> sensor;

Diethyl ether sensor

## Abstract

Herein, carbon dots (CDs) as biocompatible, fluorescent carbon-based nanomaterials were synthesized from papaya seed waste as renewable carbon sources for the first time via a facile acid pyrolysis method. The papaya seed-derived CDs showed blue fluorescence emission under UV light (365 nm) with a quantum yield of 2.74%, and contained oxygen-, and nitrogen- containing functional groups. Due to their surface functionality, the CDs have a great potential for using as fluorescence sensing probe in metal ion sensing application. The CD solution exhibited the most selective detection to Cu<sup>2+</sup> as presented the highest fluorescence quenching with the limit of detection (LOD) of 5.16 μM. The CD-paper-based fluorescent sensor was also developed for practical application, and the RGB value was used to compare the sensitivity of CDs toward metal ions. The CD sensing film was also prepared for diethyl ether vapor sensing via optical electronic nose system. The principal component analysis (PCA) score plots revealed the total variance of 99.3%, indicating that the CDs can be used to discriminate different concentrations of diethyl ether/ethanol vapor mixtures. This work demonstrated that the papaya seed-derived CDs have a great attention to be alternative materials for developing sensing materials in both solution and film forms.

## 1. Introduction

Carbon dots (CDs) are small carbon-based nanomaterials that have attracted considerable attention in recent years due to their unique optical and electrical properties, biocompatibility, low toxicity, high water solubility, high photostability and surface functionality [1-3]. CDs can be synthesized from various carbon sources, and it is normally prepared via simple thermal treatment including pyrolysis, hydrothermal treatment, and microwave method with the presence of acid for dehydration process [4]. Nowadays, the synthesis of CDs from plant, animal, or industrial wastes has drawn an attention not only because it is cost-effectiveness and readily available but the recycling of natural resources also has the potential to reduce their negative effects on the environment, such as fruit wastes, biomass, and tree leaves [5,6]. For example, Tyagi *et al.* reported the preparation of CDs from lemon peel waste using a hydrothermal treatment [7]. In Thailand, papaya (*Carica papaya*) is one of the most widely consumed fruits normally found everywhere and all year round because of its ease of cultivation in every part of Thailand. Thai people usually use both unripe and ripe papaya in a variety of Thai traditional dishes. For instance, ripe papaya is used as a main ingredient for

cooking traditional Thai papaya salad called “Som Tam”, which is famous all over the world. As a result, papaya peels and seeds are always discarded as food wastes in virtually all Thai local markets. Papaya seed comprises of significant amounts of proteins (28%), lipids (28%) and crude fiber (22%) [8]. However, there have never been previously reported about the utilization of papaya seed as a carbon source for the CD synthesis. The papaya seed is thus a good candidate as a carbon source for CD preparation in this work.

Due to their unique absorption and fluorescence emission properties and biocompatibility, the CDs are considered as alternative materials for a variety of applications such as bioimaging, drug deliver, photocatalysis, energy harvesting and sensing [9-11]. The detection of toxic ions in the environment is a crucial topic in these days, especially heavy metal ions, because they are widely used in various processes such as copper (Cu<sup>2+</sup>), chromium (Cr<sup>6+</sup>), lead (Pb<sup>2+</sup>) and mercury (Hg<sup>2+</sup>) ions. Copper ions (Cu<sup>2+</sup>) play a crucial role in many biological and environmental processes and are widely used in various industrial processes [12,13]. Even if Cu<sup>2+</sup> does not have a hazard effect on human body at normal conditions, consuming more than the recommended daily quantity is harmful to human health since it can cause the human genetic disorder called “Wilson disease” [14]. Copper ion

sensing is therefore important for various applications, such as water quality control, food safety, medical diagnosis, and environmental monitoring [13]. There have been many reports developed different techniques for the detection of  $\text{Cu}^{2+}$  including electrochemical sensors, optical sensors, and other conventional methods like inductively coupled plasma mass spectrometry (ICP-MS) and atomic absorption spectroscopy (AAS) [13,15,16]. However, the convention techniques usually require multi-step sample preparation and complex instruments, not suitable for practical usage. The optical sensor such as fluorescent probe is thus an efficient method for sensing metal ion in real applications. As CDs contain oxygen and nitrogen-rich functional groups, it is also a great potential to bind with specific metal ion and present the change in optical phenomena for the detection of metal ion [17].

Not only metal ions can cause a hazard effect to human health and environment, volatile organic compounds (VOCs) can also cause a variety of health effects including respiratory irritation and damage to human organ. Diethyl ether is a flammable liquid which can vaporize under normal condition. It has been applied in a variety of industrial processes e.g. fuel, pharmaceutical, and explosive material industries [18,19]. Nonetheless, long-term exposure of diethyl ether in low concentration can cause headache, fatigue, nausea, and other related symptoms in human [20]. Diethyl ether is typically produced by dehydrating ethanol via Barbet process in the presence of acid catalyst [21]. The efficient sensing to distinguish the ethanol and diethyl ether can provide many benefits for both environmental and industrial impacts.

Gas chromatography (GC) is typically used to measure the presence of diethyl ether or other VOCs [22]. However, this approach is not portable due to a lot of instruments required. Optical electronic nose can be a better choice for detecting the analyte in vapor phase for practical applications. Electronic nose is an artificial equipment used to mimic an olfactory function in human to differentiate volatile compounds in vapor phase with different sensitivity of sensing materials [23]. There are several functions of electronic nose for instance, optical and electrical electronic nose. Optical electronic nose system integrated with CDs for volatile organic compounds (VOCs) sensing have been reported [24-26]. For example, Supchocksoonthorn *et al.* prepared black sesame seed-derived CD thin film for ammonia detection via optical electronic nose system as the as-prepared CD could form

a stable complex due to the high polarity of CDs [27]. As shown in previous reports, the CDs-integrated with electronic nose were normally sensitive to high polar VOCs due to their hydrophilic functional group interaction on the surface. The preparation of CD sensing film for the detection of low polar VOCs like diethyl ether is thus beneficial for environmental monitoring sensor.

In this work, the CDs prepared from sustainable, renewable papaya seed waste were applied as sensing materials in both solution and vapor phases. In solution phase, the CD solution was used to sense  $\text{Cu}^{2+}$  and the CD coated paper sensor was also demonstrated for practical applications. Furthermore, the CDs were prepared as sensing layer to consolidate with optical electronic nose system for the detection of diethyl ether in vapor phase. Principle component analysis (PCA) is a statistical technique for reducing several dimensional data into an array of linearly uncorrelated variable values called principal components (PC) [28,29]. It is therefore widely utilized in gas sensing studies that sought to categorize various kinds of data. Herein, the PCA was thus applied to observe the gas sensing abilities of the CDs to distinguish different diethyl ether concentrations from various light source data. This report not only serves the development of CD synthesis from new, sustainable precursor, but also enlarge the practical applications of CDs via its unique optical properties to be other essential possibility for the detection of metal ion in solution phase and VOCs in vapor phase (Figure 1).

## 2. Experimental

### 2.1 Materials and chemicals

Papaya seeds were collected from Khaek Dam papaya with orange-colored skin, a traditional papaya cultivar in Thailand, and obtained from a local market in Muang, Lop Buri, Thailand. All chemicals were purchased from Sigma-Aldrich and used without further purification. 65% Nitric acid ( $\text{HNO}_3$ ), 98% sulfuric acid ( $\text{H}_2\text{SO}_4$ ), sodium hydroxide (NaOH) pellets and diethyl ether were bought from Carlo Erba. Cellulose dialysis membrane with MWCO 1kDa (Spectrum Labs) was used to purify the CD solution. All experiments were conducted using deionized water with resistance of 15M $\Omega$ .

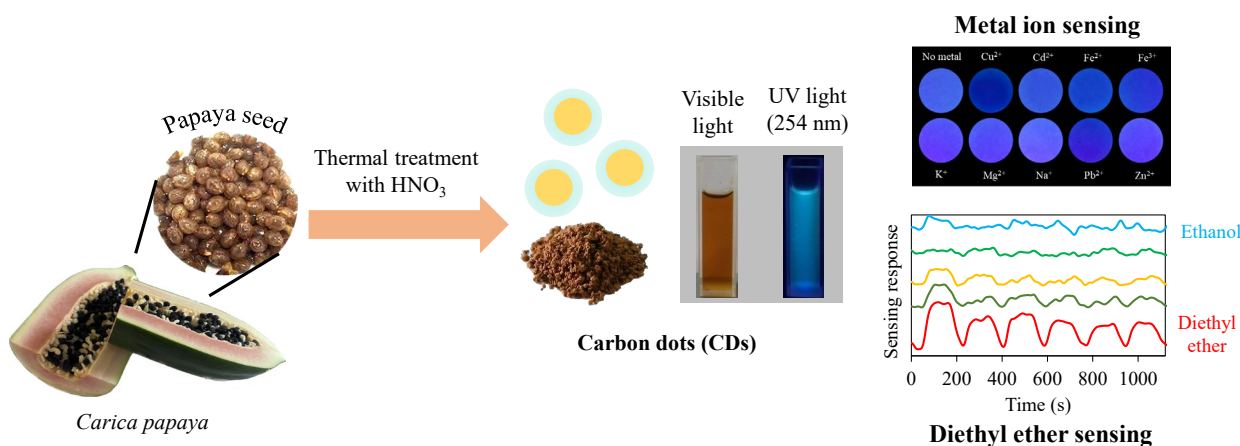


**Figure 1.** Schematic illustration of papaya seed-derived CD synthesis and applications.

## 2.2 Synthesis of CDs from papaya seed waste

Papaya seeds were cleaned with tap water and deionized water, respectively, and then dried at 80°C to 100°C in the oven for at least 12 h. The dried papaya seeds were then ground into powder using a household blender. The papaya seed powder (20 g) was mixed with 2.5 M HNO<sub>3</sub> (50 mL) and then transferred the mixture to a crucible dish. The mixture was heated at 250°C for 6 h in a furnace to produce the carbon nanoparticles. After the reaction completed, the mixture was cooled to room temperature, and then filtered to remove the residues. The pH of the solution was then adjusted to neutrality with 10%w/v NaOH, and then dialyzed against deionized water for three days to remove unreacted reagents. To remove the large particles, the CD solution was centrifuged at 10,000 rpm for 30 min before using in other experiments.

## 2.3 Characterizations

UV-Vis spectrophotometer (Shimadzu, UV-1700 PharmaSpec) and fluorescence spectrometer (Jasco, FP-6200) were used to investigate the absorption and fluorescence emission properties of the CD solution. Size and morphology of CDs were characterized using a high-resolution transmission electron microscope (HR-TEM; Tecnai G2 F20, FEI Corporation). The structural characterizations were studied using a Fourier transform infrared (FT-IR) spectrometer (Perkin Elmer, Spectrum 2000) with KBr pellets, and an X-ray photoelectron spectrometer (XPS; AXIS ULTRADLD, Kratos analytical, Manchester, UK) with monochromatic Al K<sub>α1,2</sub> radiation at 1.4 keV.

Quantum yield measurement was carried out by measuring the absorbance and fluorescence emission of CD solution compared with a quinine sulphate in 0.1 M H<sub>2</sub>SO<sub>4</sub> solution as a reference fluorescence dye ( $\Phi_R=0.54=54\%$ ). The quantum yield can be calculated using Equation (1);

$$\Phi_{CD} = \Phi_R \times \frac{I_{CD}}{I_R} \times \frac{A_R}{A_{CD}} \times \frac{n_{CD}^2}{n_R^2} \quad (1)$$

where  $\Phi$  is the quantum yield,  $I$  is the fluorescence intensity,  $A$  is the absorbance and  $n$  is the refractive index of the solvent. The subscript "R" refers as the quinine sulphate reference solution, whereas the subscript "CD" refers as the CD solution [30].

## 2.4 Metal ion sensing and paper-based metal ion sensing

1.5 mL of 50 μM different metal ion solutions (Cu<sup>2+</sup>, Pb<sup>2+</sup>, Fe<sup>2+</sup>, Fe<sup>3+</sup>, Cd<sup>2+</sup>, K<sup>+</sup>, Mg<sup>2+</sup>, Zn<sup>2+</sup>, and Na<sup>+</sup>) were homogeneously mixed with 3.5 mL of 0.02 g·L<sup>-1</sup> CD solution. The fluorescence spectra at 360 nm excitation were then measured to study the selectivity of CDs toward metal ions.

To fabricate the paper-based sensor for metal ion detection, the cellulose filter paper (Whatman No.1) was immersed with the CD solution (0.1 g·L<sup>-1</sup>) until the CD solution fully covered the paper. After that, the paper was then dried in the hot oven at 80°C for 3 h

before dropping metal ion solution for the detection test. The fluorescence quenching of CD-paper sensor was observed under UV light (365 nm). The sum of RGB (Red, Green and Blue) values of each metal ion spot on the paper-based sensor was analyzed from Paint program (Microsoft 11) to distinguish the different in selectivity of CD toward different metal ions and different concentrations of Cu<sup>2+</sup>. All photos were taken by an iPhone 6 camera in a black box to reduce the light interference from surrounding. The sum of RGB values was calculated from the average of RGB values using 10 different spots on the paper sensor area, mostly at the center of paper.

## 2.5 Diethyl ether vapor sensing using optical electronic nose system

1 mL of CD aqueous solution (25 g·L<sup>-1</sup>) was drop-casted to the cleaned glass substrate with the size of 2.5 cm × 2.5 cm, and then dried in an oven at 80°C for 12 h to prepare a sensing film for vapor detection using optical electronic nose system. Diethyl ether vapor was detected using a home-made optical electronic nose system comprising CD thin film as a sensing layer. There are eight different light sources in the system. The change in sensing signal after flowing the analyte vapor compared with that of the reference gas (99.99% N<sub>2</sub> gas) was recorded as light transmission intensity through the CD film using photodetector. More details about electronic nose set up were reported in related previous works [24,31]. A multiple gas sensing response data was collected from a data acquisition card as light transmission through the CD film from 8 different light sources. The LabVIEW program was then used to analyze the gas sensing response and perform the PCA analysis.

## 3. Results and discussion

### 3.1 Structural and morphology analysis of papaya seed-derived CDs

Structural characterization of the papaya seed-derived CDs was carried out using FT-IR spectroscopy and XPS. The O-H/N-H stretching (3400 cm<sup>-1</sup>), C-H stretching (2866 cm<sup>-1</sup> to 2939 cm<sup>-1</sup>), C=O/C=C stretching (1628 cm<sup>-1</sup> to 1719 cm<sup>-1</sup>), and C-O stretching (1112 cm<sup>-1</sup>) in the FT-IR spectrum (Figure 2(a)) indicated the presence of oxygen/nitrogen containing groups on the CD surface that contributed to hydrophilic properties of the as-prepared CDs. The survey XPS spectrum (Figure 2(b)) revealed the elemental composition of CDs with the existence of O<sub>1s</sub> (531 eV), N<sub>1s</sub> (399 eV), and C<sub>1s</sub> (285 eV) peaks with the atomic concentration of 19.78%, 9.79%, and 67.58%, respectively. The high resolution of C<sub>1s</sub> peak (Figure 2(c)) confirmed C=C/C-C, C-N, C-O, and C=O at 284.9, 285.2, 286.4, and 288.2 eV, respectively [32], which is relatively consistent with the FT-IR results. Furthermore, the N<sub>1s</sub> high resolution peak (Figure 2(d)) showed that the CDs contained three different nitrogen bonding modes, including pyridinic (399 eV), pyrrolic (400.1 eV), and graphitic nitrogen (401.5 eV). As the papaya seed consists of a large amount of proteins, these led to the formation of various nitrogen-containing groups on the CD surface via dehydration and carbonization processes.

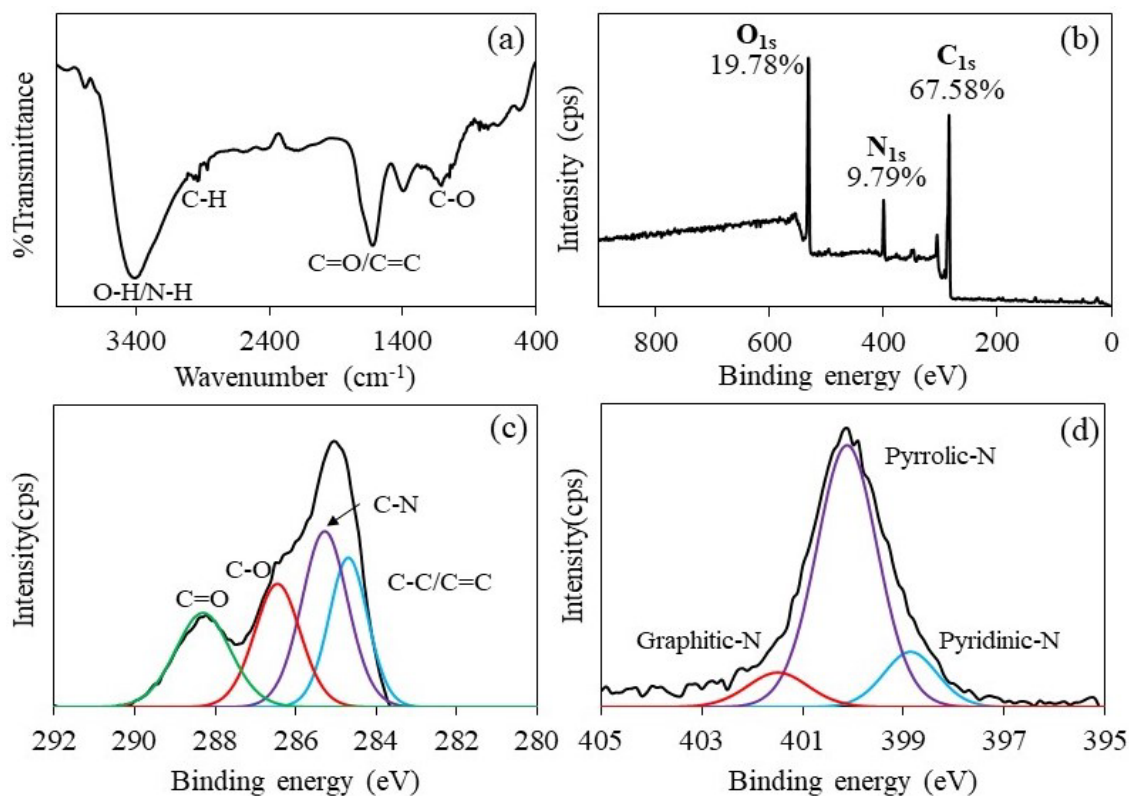


**Figure 2.** (a) FT-IR spectrum, (b) survey XPS spectrum, (c)  $C_{1s}$ , and (d)  $N_{1s}$  high-resolution peaks of the papaya seed-derived CDs.

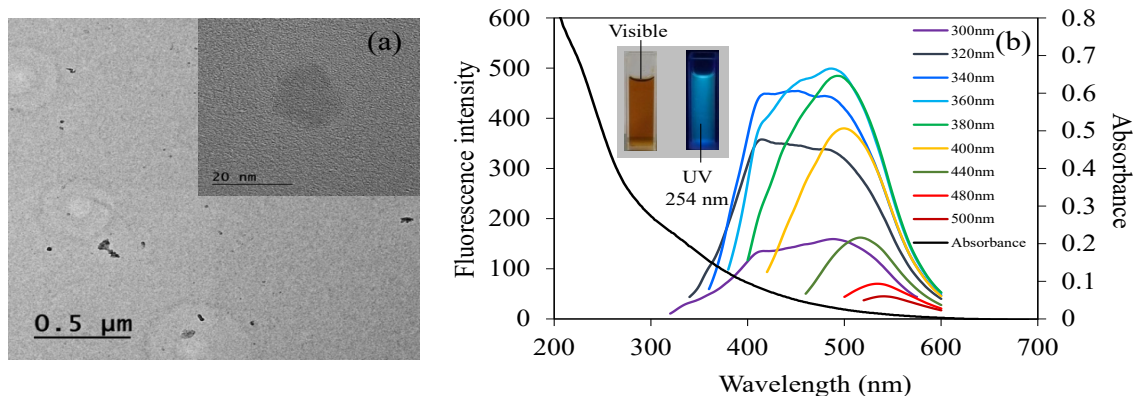


**Figure 3.** (a) HR-TEM images, and (b) UV-Vis absorption spectrum and fluorescent emission spectra of the papaya seed-derived CDs.

HR-TEM was used to examine the size and shape of the as-synthesized CDs obtained from papaya seeds. The HR-TEM images (Figure 3(a)) showed the virtually spherical shape of CDs with the average diameter of 20 nm, indicating that the large size of CDs presented in the images may be due to the agglomeration of CD particles. These results could be confirmed by the zeta potential value of 0.4 mV.

### 3.2 Optical properties of CDs

UV-Vis absorption spectrum (Figure 3(b)) exhibited two broad peaks, indicating the presence of  $\pi-\pi^*$  transition of C=C (250 nm to 300 nm) and  $n-\pi^*$  transition of C=O (350 nm to 380 nm). The CD solution emitted blue fluorescence upon UV irradiation of 365 nm as shown in the inset of Figure 3(b). The fluorescent emission spectra

(Figure 3(b)) were recorded using different excitation wavelengths from 300 nm to 500 nm. The excitation-dependent emission was observed which can be ascribed from the different emissive sites from various surface functional groups on the CDs [33]. The strongest emission intensity was observed at 491 nm when the 360 nm excitation was applied. The quantum yield was calculated to be 2.74% when the quinine sulphate was used as a reference.

The fluorescence and absorption stability of the CDs were analyzed under ambient conditions for 7 weeks and UV exposure (365 nm) for 360 min (Figure 4(a-b)). The UV-Vis absorbance and fluorescent intensity of the CD solution demonstrated high stability upon visible light as remained about 100%. After the UV irradiation at 360 nm, they also exhibited almost 100% for absorbance retention, and 85% for fluorescence retention. These results indicated the high photostability and the excellent resistance to photobleaching of the CDs.

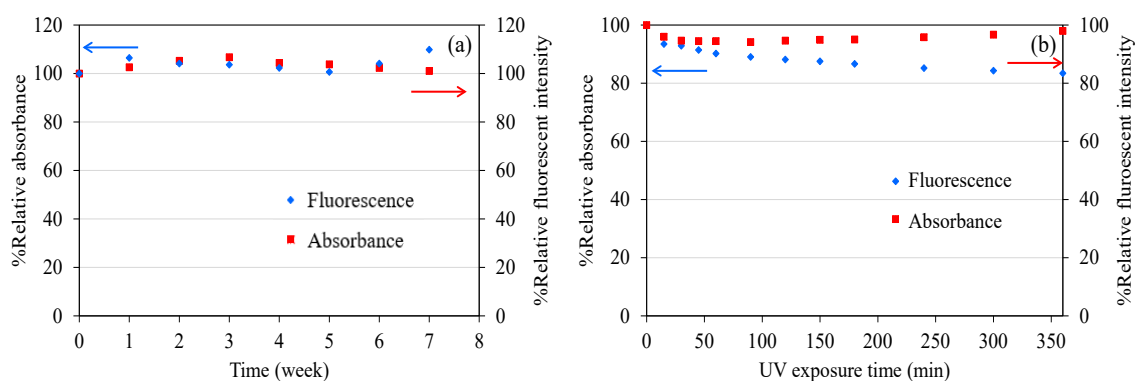


**Figure 4.** Relative fluorescent and absorbance intensity of CDs (a) under ambient conditions for 7 weeks, and (b) after UV exposure (365 nm) for 360 min.

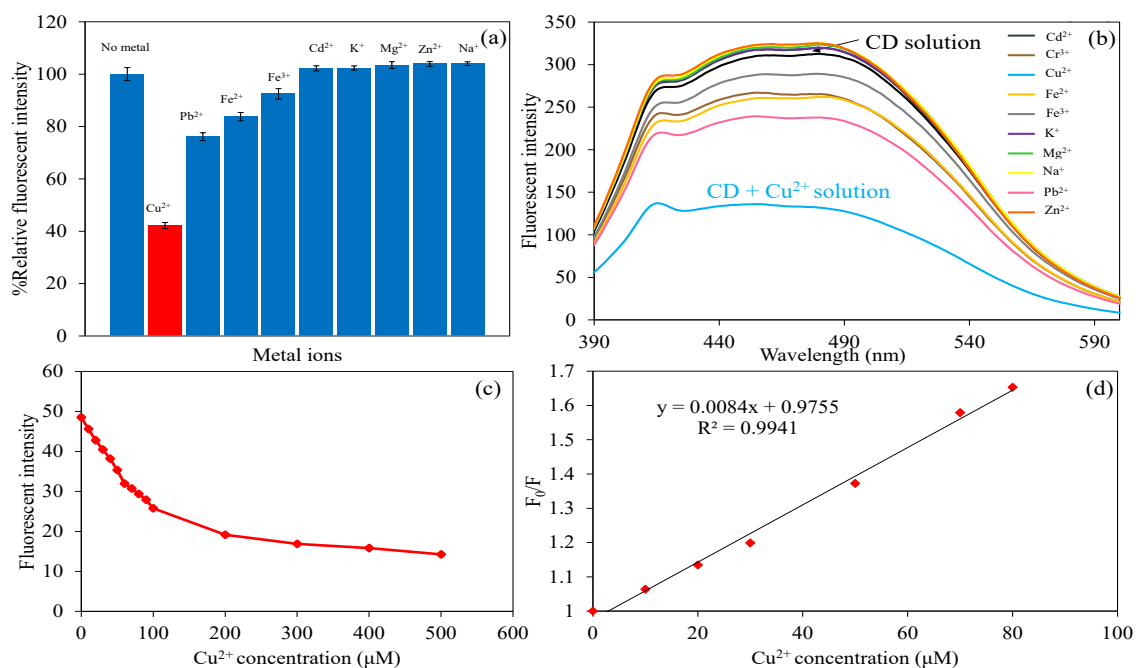


**Figure 5.** (a) Relative fluorescent intensity and (b) fluorescent spectra of CD solution with the addition of various metal ions, (c) the fluorescent intensity of CDs after addition of Cu<sup>2+</sup> in the concentration of 0 to 500 μM, and (d) Stern-Volmer plot for LOD calculation where F<sub>0</sub> is the initial fluorescent intensity and F is the fluorescent intensity of CD solution after mixing with Cu<sup>2+</sup> in different concentrations.

### 3.3 Metal ion sensing

The selectivity of CD fluorescent sensing toward different types of metal ions were tested by mixing the CD solution with each metal ion solution, including Cu<sup>2+</sup>, Pb<sup>2+</sup>, Fe<sup>2+</sup>, Fe<sup>3+</sup>, Cd<sup>2+</sup>, K<sup>+</sup>, Mg<sup>2+</sup>, Zn<sup>2+</sup> and Na<sup>+</sup>. As shown in Figure 5(a-b), the highest reduction of fluorescent intensity of about 60% was observed when the Cu<sup>2+</sup> was added to the CD solution, suggesting the highest sensitivity of CDs for Cu<sup>2+</sup> detection. This may be because the presence of nitrogen-containing groups on the CD surface could form the chelation with Cu<sup>2+</sup> faster than other ions, inducing the fluorescent quenching phenomenon [34,35]. In addition, the concentrations of Cu<sup>2+</sup> were varied from 0 μM to 500 μM (Figure 5(c)). It was found that the reduction of fluorescent intensity dramatically increased when the Cu<sup>2+</sup> concentration was in the range from 0 μM to 100 μM, and became stable after adding 200 μM of Cu<sup>2+</sup>. According to this maximum adsorption of Cu<sup>2+</sup> on CD, the surface coverage of the CD particle was calculated to be 7.78 ions nm<sup>-2</sup>, and the adsorption capacity for Cu<sup>2+</sup> with CDs

was determined to be 109.1 mg.g<sup>-1</sup>. These results suggested that the CDs can also act as a high-performance adsorbent for Cu<sup>2+</sup> adsorption (the calculation is presented in Supplementary Information). Limit of detection (LOD) was also calculated using Stern-Volmer equation (LOD = 3S.D.) as shown in Figure 5(d). The LOD of Cu<sup>2+</sup> sensing was found to be 5.14 μM, which is relatively efficient to detect Cu<sup>2+</sup> in practical applications.

The fabrication of paper-based fluorescent CD for metal ion sensor was developed (Figure 6(a-b)). The metal ion solution (50 μM) was dropped onto the CD paper sensor at designated area, and the photo was taken under UV irradiation (365 nm). The result was consistent with the fluorescent quenching found in the fluorescent spectra. The Cu<sup>2+</sup> area was observed to be the darkest as the fluorescent intensity of CDs decreased which can be confirmed by the highest reduction of RGB value (Figure 6(c)). The different concentration of Cu<sup>2+</sup> was also used to test the paper-based CD sensor performance. The higher the concentration of Cu<sup>2+</sup>, the lower the RGB values observed, consistent with the fluorescent results (Figure 6(d)).



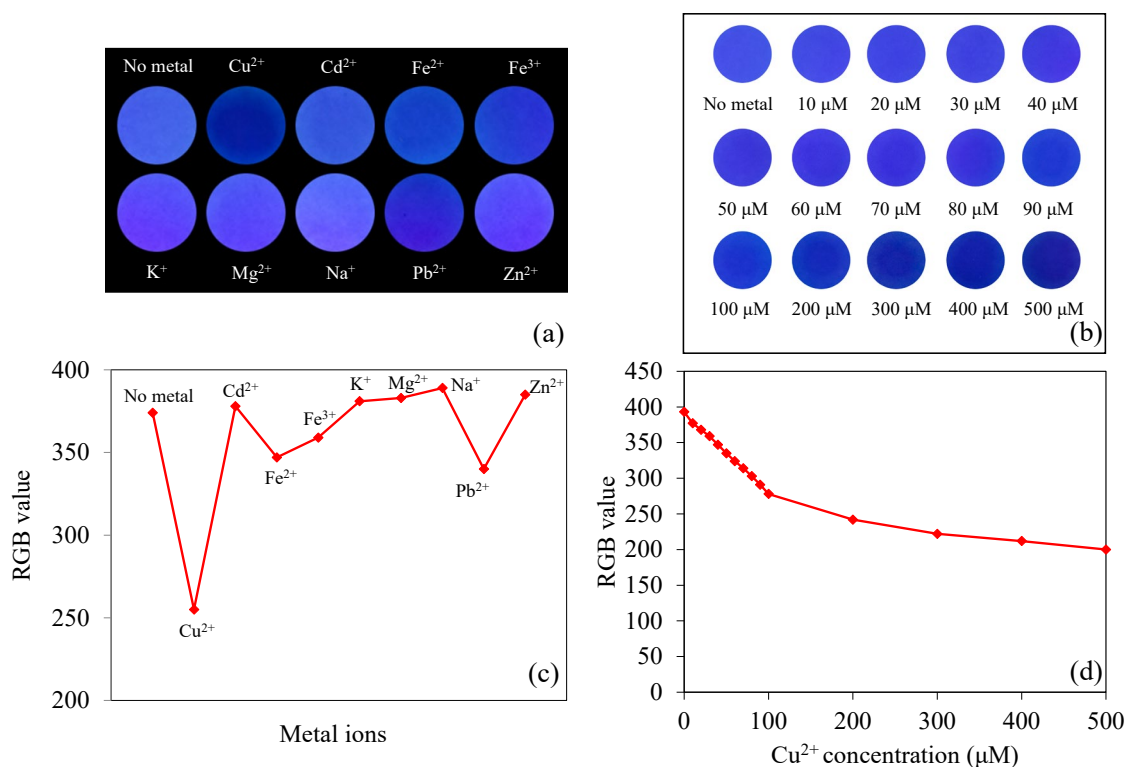


**Figure 6.** The image of paper-based CD sensor (a) after dropping various metal ions and (b) different Cu<sup>2+</sup> concentrations under UV lamp (365 nm), (c) the sum of RGB value at different area of CD paper with the presence of different metal ions, and (d) the sum of RGB value of CD paper with the presence of different Cu<sup>2+</sup> concentrations.

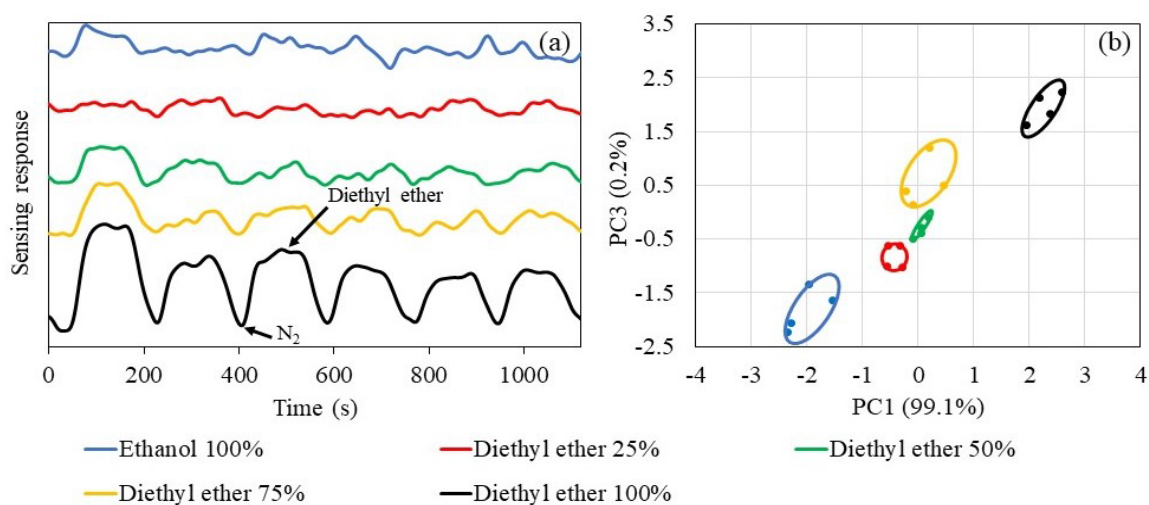


**Figure 7.** (a) Sensing response of CD sensing film upon different concentrations of diethyl ether and ethanol vapor under white light source and (b) PCA score plots of different concentrations of diethyl ether and ethanol

### 3.4 Diethyl ether sensing via optical electronic nose system

The CD sensing film was integrated with the optical electronic nose system for the detection of diethyl ether in vapor phase. In the system, the different LED light sources were alternatively illuminated through the CD film, and the sensing response was detected in term of light transmission through the CD film as a function of time. Nitrogen gas was used as reference and carrier gas, and the flow of sample vapor was switched on and off repeatedly to observe the

change of light transmission. The gas sensing response depicted the dramatically increase of light transmission intensity when the diethyl ether vapor was flowed, and the signal dropped and returned to its original intensity when the nitrogen gas flow was switched (Figure 7(a)). These results suggested that the CD can be used to prepare a sensing film for the detection of diethyl ether in electronic nose system. The repeatability and reproducibility of the sensing cycle indicated the physical interaction between CD and diethyl ether vapor. On the other hand, the change of sensing signal was relatively small upon

ethanol vapor flowing due to the lower sensitivity of CD toward ethanol vapor. As the diethyl ether is normally produced from ethanol in industrial process, the effects of the diethyl ether concentration in ethanol solution to the sensing response were also studied. The results showed that the change of light transmission intensity decreased when the ratio of ethanol was increased. This could be described from the computation studies reported in our previous works [25]. Even though the diethyl ether has low polarity than the ethanol, the diethyl ether structure contains more C-H bonding which could form greater C-H- $\pi$  interaction with sp<sup>2</sup>-graphitic structure of CD core, leading to the higher sensitivity of CD with diethyl ether vapor compared with that of ethanol. The electron transfer between diethyl ether molecules and CDs, and the change in energy band gap could be the cause of the optical modulation of the CDs after exposure to diethyl ether [36,37]. The sensing response from eight light sources were collected to perform the principal component analysis (PCA). The PCA two-dimensional score plot (Figure 7(b)) displayed no overlap of each cluster from different concentrations of diethyl ether in ethanol solution with total variance of 99.3%, indicating that the CD film has a great potential to be a sensing layer for discriminating diethyl ether and ethanol.

#### 4. Conclusions

In this work, the papaya seed waste was used as a precursor for CD synthesis via simple, facile thermal treatment for the first time. The as-prepared CDs were demonstrated as fluorescent sensing for Cu<sup>2+</sup> detection with the LOD of 5.14  $\mu$ M. The paper-based fluorescent sensor for metal ion detection was also developed for more practical use. In addition, the CD sensing film was prepared to incorporate with optical electronic nose system for diethyl ether detection in vapor phase. The PCA plot revealed that the CD can be used to distinguish the diethyl ether with the presence of different amounts of ethanol. These results imply that the CDs would be a great alternative sensing materials for the detection of analytes in both solution and vapor phases.

#### Acknowledgements

This work is supported by the funding under Thammasat University Research Unit in Carbon Materials and Green Chemistry Innovations. The authors also would like to acknowledge the Central Scientific Instrument Center (CSIC), Thammasat University Center of Scientific Equipment for Advanced Research (TUCSEAR), and Department of Chemistry, Faculty of Science and Technology, Thammasat University.

#### References

- [1] D. Zhong, H. Miao, K. Yang, and X. Yang, "Carbon dots originated from carnation for fluorescent and colorimetric pH sensing," *Materials Letters*, vol. 166, pp. 89-92, 2016.
- [2] J. Liu, R. Li, and B. Yang, "Carbon dots: A new type of carbon-based nanomaterial with wide applications," *ACS Central Science*, vol. 6, no. 12, pp. 2179-2195, 2020.
- [3] P. Zhao, and L. Zhu, "Dispersibility of carbon dots in aqueous and/or organic solvents," *Chemical Communications*, vol. 54, no. 43, pp. 5401-5406, 2018.
- [4] P.-C. Hsu, and H.-T. Chang, "Synthesis of high-quality carbon nanodots from hydrophilic compounds: role of functional groups," *Chemical Communications*, vol. 48, no. 33, pp. 3984-3986, 2012.
- [5] B. P. de Oliveira, and F. O. M. da Silva Abreu, "Carbon quantum dots synthesis from waste and by-products: Perspectives and challenges," *Materials Letters*, vol. 282, p. 128764, 2021.
- [6] N. K. Khairol Anuar, H. L. Tan, Y. P. Lim, M. S. So'aib, and N. F. Abu Bakar, "A review on multifunctional carbon-dots synthesized from biomass waste: Design/fabrication, characterization and applications," *Frontiers in Energy Research*, vol. 9, pp. 1-22, 2021.
- [7] A. Tyagi, K. M. Tripathi, N. Singh, S. Choudhary, and R. K. Gupta, "Green synthesis of carbon quantum dots from lemon peel waste: Applications in sensing and photocatalysis," *RSC Advances*, vol. 6, no. 76, pp. 72423-72432, 2016.
- [8] E. K. Marfo, O. L. Oke, and O. A. Afolabi, "Chemical composition of papaya (*Carica papaya*) seeds," *Food Chemistry*, vol. 22, no. 4, pp. 259-266, 1986.
- [9] R. M. S. Sendão, J. C. G. Esteves da Silva, and L. Pinto da Silva, "Applications of fluorescent carbon dots as photocatalysts: A Review," *Catalysts*, vol. 13, no. 1, 2023.
- [10] B. Wang, H. Cai, G. I. N. Waterhouse, X. Qu, B. Yang, and S. Lu, "Carbon dots in bioimaging, biosensing and therapeutics: A comprehensive review," *Small Science*, vol. 2, no. 6, p. 2200012, 2022.
- [11] L. Wang, Y. Wang, H. Wang, G. Xu, A. Döring, W. A. Daoud, J. Xu, A. L. Rogach, Y. Xi, and Y. Zi, "Carbon dot-based composite films for simultaneously harvesting raindrop energy and boosting solar energy conversion efficiency in hybrid cells," *ACS Nano*, vol. 14, no. 8, pp. 10359-10369, 2020.
- [12] R. A. Festa, and D. J. Thiele, "Copper: an essential metal in biology," *Current Biology*, vol. 21, no. 21, pp. R877-83, 2011.
- [13] Z. Gerdan, Y. Saylan, and A. Denizli, "Recent advances of optical sensors for copper ion detection," *Micromachines (Basel)*, vol. 13, no. 8, 2022.
- [14] Z. Zhu, R. McKendry, and C. L. Chavez, "Chapter 20 - Signaling in Copper Ion Homeostasis," in *Cell and Molecular Response to Stress*, vol. 1, K. B. Storey and J. M. Storey Eds.: Elsevier, 2000, pp. 293-300.
- [15] P. Jungová, J. Navrátilová, O. Peš, T. Vaculovič, V. Kanický, J. Šmarda, and J. Preisler, "Substrate-assisted laser desorption inductively-coupled plasma mass spectrometry for determination of copper in myeloid leukemia cells," *Journal of Analytical Atomic Spectrometry*, vol. 25, no. 5, pp. 662-668, 2010.
- [16] T. Wu, T. Xu, and Z. Ma, "Sensitive electrochemical detection of copper ions based on the copper(ii) ion assisted etching of Au@Ag nanoparticles," *Analyst*, vol. 140, no. 23, pp. 8041-8047, 2015.
- [17] K. Patir, and S. K. Gogoi, "Nitrogen-doped carbon dots as fluorescence ON-OFF-ON sensor for parallel detection of copper(II) and mercury(II) ions in solutions as well as in filter

- paper-based microfluidic device," *Nanoscale Advances*, vol. 1, no. 2, pp. 592-601, 2019.
- [18] A. Ibrahim, "Investigating the effect of using diethyl ether as a fuel additive on diesel engine performance and combustion," *Applied Thermal Engineering*, vol. 107, pp. 853-862, 2016.
- [19] T. K. Phung and G. Busca, "Diethyl ether cracking and ethanol dehydration: Acid catalysis and reaction paths," *Chemical Engineering Journal*, vol. 272, pp. 92-101, 2015.
- [20] W. Zhang, F. Yang, B. Liu, and K. Zhou, "Novel diethyl ether gas sensor based on cataluminescence on Nano-Pd/ZnNi<sub>3</sub>Al<sub>2</sub>O<sub>7</sub>," *ACS Omega*, vol. 6, no. 27, pp. 17576-17583, 2021.
- [21] R. Alviany, A. Wahyudi, I. Gunardi, A. Roesyadi, F. Kurniawansyah, and D. Hari Prajitno, "Diethyl ether production as a substitute for gasoline," *MATEC Web of Conferences*, vol. 156, p. 06003, 2018.
- [22] F. Pan, B. Sun, Z. Tang, and S. Zhu, "A fast response cataluminescence ether gas sensor based on GO/Mo<sub>2</sub>TiC<sub>2</sub>T<sub>x</sub> at low working temperature," *RSC Advances*, vol. 12, no. 14, pp. 8361-8367, 2022.
- [23] T. Arakawa, K. Itani, K. Toma, and K. Mitsubayashi, "Biosensors: Gas Sensors," in *Encyclopedia of Sensors and Biosensors*, R. Narayan Ed., First ed. Oxford: Elsevier, 2023, pp. 478-504.
- [24] M. R. Pacquiao, M. D. G. de Luna, N. Thongsai, S. Kladsomboon, and P. Paoprasert, "Highly fluorescent carbon dots from enokitake mushroom as multi-faceted optical nanomaterials for Cr<sup>6+</sup> and VOC detection and imaging applications," *Applied Surface Science*, vol. 453, pp. 192-203, 2018.
- [25] N. Thongsai, P. Jaiyong, S. Kladsomboon, I. In, and P. Paoprasert, "Utilization of carbon dots from jackfruit for real-time sensing of acetone vapor and understanding the electronic and interfacial interactions using density functional theory," *Applied Surface Science*, vol. 487, pp. 1233-1244, 2019.
- [26] N. Thongsai, N. Tanawannapong, J. Praneerad, S. Kladsomboon, P. Jaiyong, and P. Paoprasert, "Real-time detection of alcohol vapors and volatile organic compounds via optical electronic nose using carbon dots prepared from rice husk and density functional theory calculation," *Colloids and Surfaces A: Physicochemical and Engineering Aspects*, vol. 560, pp. 278-287, 2019.
- [27] P. Supchocksoonthorn, N. Thongsai, H. Moonmuang, S. Kladsomboon, P. Jaiyong, and P. Paoprasert, "Label-free carbon dots from black sesame seeds for real-time detection of ammonia vapor via optical electronic nose and density functional theory calculation," *Colloids and Surfaces A: Physicochemical and Engineering Aspects*, vol. 575, pp. 118-128, 2019.
- [28] S. Bedoui, R. Faleh, H. Samet, and A. Kachouri, *Electronic nose system and principal component analysis technique for gases identification*. 2013, pp. 1-6.
- [29] I. T. Jolliffe, and J. Cadima, "Principal component analysis: a review and recent developments," *Philos Trans A Math Phys Eng Sci*, vol. 374, no. 2065, p. 20150202, 2016.
- [30] F. Lu, S. Yang, Y. Song, C. Zhai, Q. Wang, G. Ding, and Z. Kang, "Hydroxyl functionalized carbon dots with strong radical scavenging ability promote cell proliferation," *Materials Research Express*, vol. 6, no. 6, p. 065030, 2019.
- [31] S. Kladsomboon, M. Lutz, T. Pogfay, T. Puntheeranurak, and T. Kerdcharoen, "Hybrid optical-electrochemical electronic nose system based on Zn-porphyrin and multi-walled carbon nanotube composite," *Journal of Nanoscience and Nanotechnology*, vol. 12, no. 7, pp. 5240-5244, 2012.
- [32] X. Ma, S. Li, V. Hessel, L. Lin, S. Meskers, and F. Gallucci, "Synthesis of luminescent carbon quantum dots by microplasma process," *Chemical Engineering and Processing - Process Intensification*, vol. 140, pp. 29-35, 2019.
- [33] M. Fu, F. Ehrat, Y. Wang, K. Z. Milowska, C. Reckmeier, A. L. Rogach, J. K. Stolarczyk, A. S. Urban, and J. Feldmann, "Carbon dots: A unique fluorescent cocktail of polycyclic aromatic hydrocarbons," *Nano Letters*, vol. 15, no. 9, pp. 6030-6035, 2015.
- [34] L. Zhao, H. Li, Y. Xu, H. Liu, T. Zhou, N. Huang, Y. Li, and L. Ding, "Selective detection of copper ion in complex real samples based on nitrogen-doped carbon quantum dots," *Analytical and Bioanalytical Chemistry*, vol. 410, no. 18, pp. 4301-4309, 2018.
- [35] M. Ganiga, and J. Cyriac, "Understanding the photoluminescence mechanism of nitrogen-doped carbon dots by selective interaction with copper ions," *ChemPhysChem*, vol. 17, no. 15, pp. 2315-2321, 2016.
- [36] R. Palasuek, S. Kladsomboon, T. Thepudom, and T. Kerdcharoen, "Optical electronic nose based on porphyrin and phthalocyanine thin films for rice flavour classification," in *2014 IEEE Ninth International Conference on Intelligent Sensors, Sensor Networks and Information Processing (ISSNIP)*, 2014, pp. 1-6.
- [37] A. Pramanik, S. Biswas, and P. Kumbhakar, "Solvatochromism in highly luminescent environmental friendly carbon quantum dots for sensing applications: Conversion of bio-waste into bio-asset," *Spectrochimica Acta Part A: Molecular and Biomolecular Spectroscopy*, vol. 191, pp. 498-512, 2018.